

Homopolar Dihydrogen Bonding in Alkali Metal Amidoboranes: Crystal Engineering of Low-Dimensional Molecular Materials

David J. Wolstenholme,* Jenna Flogeras, Franklin N. Che, Andreas Decken, and G. Sean McGrady*

Department of Chemistry, University of New Brunswick, P.O. Box 4400, Fredericton, NB, Canada E3B 5A3

S Supporting Information

ABSTRACT: Hydrogen bonding is a predominant interaction in supramolecular chemistry. The absence of a conventional hydrogen bond donor in $\text{LiNMe}_2\text{BH}_3$ and KNMe_2BH_3 results in the formation of elaborate $\text{M}\cdots\text{H}-\text{B}$ polymeric arrays supported by heteropolar and homopolar $\text{H}\cdots\text{H}$ bonding, in a unique synergistic combination of unconventional intermolecular interactions.

The rational design and synthesis of solid-state architectures with low dimensionality has emerged as a central theme in supramolecular chemistry, owing to its widespread application in the preparation of novel materials with desirable physical and chemical properties.¹ In this respect, molecular recognition of complementary molecules through noncovalent interactions offers an effective means of tailoring the structures adopted by these soft materials. The two main classes of interaction employed in this endeavor are hydrogen bonding and metal–ligand coordination.¹ Conventional hydrogen bonding is characterized by a positively charged hydrogen donor interacting with an appropriate Lewis base acceptor.¹ The concept was recently expanded with the discovery of proton–hydride or dihydrogen bonding, in which a hydridic moiety rather than a nonbonding electron pair serves as the acceptor in an $\text{X}-\text{H}\cdots\text{H}-\text{Y}$ interaction.² These heteropolar dihydrogen bonds possess similar strength and directionality as their more conventional $\text{X}-\text{H}\cdots\text{Y}$ counterparts, and are similarly able to influence the structure and reactivity of a wide range of chemical systems.² Proton-hydride bonding is now a well-established phenomenon in crystal engineering and materials science.^{2e}

It is natural to invoke the involvement of proton-hydride bonding in the construction of molecular solids, owing to the strong electrostatic attraction between the oppositely charged hydrogen atoms.² However, it is counterintuitive to consider anything other than a repulsive scenario for close homopolar dihydrogen contacts. Nevertheless, nonpolar $\text{C}-\text{H}$ moieties have been shown to engage in mutually stabilizing $\text{C}-\text{H}\cdots\text{H}-\text{C}$ interactions, commonly referred to as $\text{H}-\text{H}$ bonding.³ In these instances, the partial charges associated with the hydrogen atoms are often small but not necessarily of opposite signs, confirming that homopolar dihydrogen bonding is not dominated by electrostatics, but rather does it enjoy a substantial contribution from van der Waals (VdW) attraction.^{3c} Hence, these interactions can usefully be compared with classical London dispersion forces, in which an induced dipole moment results in two fluctuating electron densities that

interact mutually to stabilize the corresponding molecular aggregate.⁴

The hierarchy of homopolar dihydrogen bonding was recently extended to include hydride–hydride interactions, after a structural and topological analysis of LiNH_2BH_3 (**1**) revealed the existence of remarkably short $\text{B}-\text{H}\cdots\text{H}-\text{B}$ contacts (2.11 Å).⁵ These were found to accumulate more electron density in the internuclear $\text{H}\cdots\text{H}$ region than their corresponding $\text{N}-\text{H}\cdots\text{H}-\text{B}$ counterparts, and a significant fraction of the hydrogen gas evolved through the thermal decomposition of **1** was shown to arise through a hydride–hydride pathway. A similar hydride–hydride reaction coordinate was subsequently revealed to be responsible for approximately half of the hydrogen gas desorbed from its parent compound ammonia-borane, NH_3BH_3 , despite the presence of only $\text{N}-\text{H}\cdots\text{H}-\text{B}$ proton–hydride bonding in its solid-state structure.⁶ These and related studies demonstrate that the intuitively destabilizing nature of homopolar dihydrogen bonding is misleading, and show that these $\text{H}\cdots\text{H}$ interactions may in fact play a silent but important role in the structure and reactivity of hydrogen-rich materials.⁷ Recent studies by two other groups have corroborated the existence of $\text{B}-\text{H}\cdots\text{H}-\text{B}$ interactions in $\text{Ca}(\text{BH}_4)_2\cdot 4\text{NH}_3/\text{Mg}(\text{BH}_4)_2$ and the gas-phase tetramer of NH_3BH_3 , and the interactions were shown to play a significant role in the desorption of hydrogen from the former species.^{8,9}

These findings have prompted us to explore the nature and consequences of homopolar dihydrogen bonding, in particular their applications in the design and synthesis of functional low-dimensional materials. Here we present a detailed description of the solid-state structures of $\text{LiNMe}_2\text{BH}_3$ (**2**) and KNMe_2BH_3 (**3**), with an emphasis on the weak $\text{B}-\text{H}\cdots\text{H}-\text{B}$ and $\text{C}-\text{H}\cdots\text{H}-\text{C}$ contacts displayed by these species (Figure 1). This

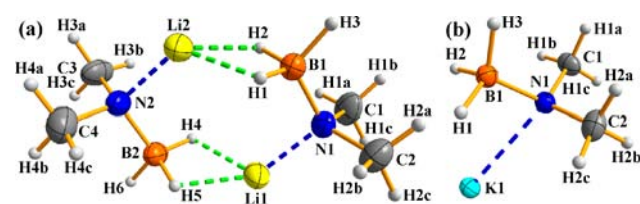


Figure 1. ORTEP view of the asymmetric units for (a) $\text{LiNMe}_2\text{BH}_3$ (**2**) and (b) KNMe_2BH_3 (**3**), with thermal ellipsoids shown at the 50% probability level for all heavy atoms.

Received: December 8, 2012

Published: January 30, 2013

structural survey has been complemented with a topological analysis of the calculated electron distribution for **2**, employing high-level periodic calculations in tandem with the concepts espoused in the quantum theory of “Atoms in Molecules” (AIM).¹⁰ This combined study has provided new insights into the important role played by homopolar dihydrogen bonding in the structural stabilization and mutual recognition of molecular hydride moieties.

The benchmark substituted borohydride **2** crystallizes in the monoclinic space group $P2_1/c$ (#14), in which its asymmetric unit consists of a MNMe_2BH_3 dimer. The structure is supported through a strong network of inter-ion $\text{Li}\cdots\text{H}-\text{B}$ and $\text{Li}\cdots\text{N}$ interactions, resulting in 1D polymeric chains that extend the solid along the c -axis of the crystal (Figure 2). This

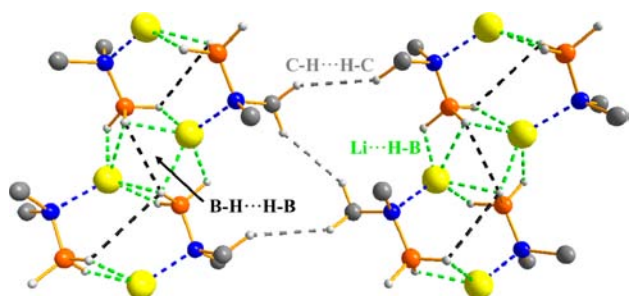


Figure 2. Extended structure of $\text{LiNMe}_2\text{BH}_3$ (**2**) viewed in the ac plane of the crystal. Salient bond lengths (Å) and angles ($^\circ$) are as follows: $\text{Li}\cdots\text{N} = 1.98$; $\text{Li}\cdots\text{H} = 1.86\text{--}2.08$; $\text{Li}\cdots\text{H}-\text{B} = 91\text{--}103$; $(\text{B})\text{H}\cdots\text{H}(\text{B}) = 2.43\text{--}2.91$; $\text{B}-\text{H}\cdots\text{H} = 106\text{--}123$; $(\text{C})\text{H}\cdots\text{H}(\text{C}) = 2.52\text{--}2.54$; $\text{C}-\text{H}\cdots\text{H} = 145\text{--}150$; $(\text{C})\text{H}\cdots\text{H}(\text{B}) = 2.67$; $\text{C}-\text{H}\cdots\text{H} = 142$; $\text{H}\cdots\text{H}-\text{B} = 140$.

packing motif closely resembles the $\text{N}-\text{H}\cdots\text{H}-\text{B}$ proton-hydride bonding present in its parent compound NHMe_2BH_3 , highlighting the comparable roles played by these different types of supramolecular interactions in stabilizing their respective solid-state structures.¹¹ This bonding scenario also invites comparison with **1**, whose smaller anion permits an additional $[\text{NH}_2\text{BH}_3]^-$ moiety to coordinate to the metal center, resulting in a pseudo-tetrahedral coordination of Li^+ ions.^{5,12} This then forces the ion pairs to orient themselves in 2D polymeric layers, rather than the 1D chains observed in **2**. The availability of $\text{N}-\text{H}$ hydrogen bond donors in **1** provides an additional means of extending its 3D structure through secondary $\text{N}-\text{H}\cdots\text{H}-\text{B}$ bonding, whereas **2** has to resort to less conventional $\text{H}\cdots\text{H}$ interactions ($\text{C}-\text{H}\cdots\text{H}-\text{B}$, $\text{C}-\text{H}\cdots\text{H}-\text{C}$, and $\text{B}-\text{H}\cdots\text{H}-\text{B}$) to bind the $[\text{NMe}_2\text{BH}_3]^-$ moieties together.

The dominant inter-ion interactions in **2** also draw several $\text{B}-\text{H}$ moieties into close enough proximity (2.43 and 2.91 Å) to facilitate $\text{B}-\text{H}\cdots\text{H}-\text{B}$ interactions. The homopolar dihydrogen contacts support a zig-zag arrangement of amidoborane anions parallel to the $\text{Li}\cdots\text{H}-\text{B}$ and $\text{Li}\cdots\text{N}$ interactions, analogous to the structural motif adopted by **1**.⁵ The similar $\text{B}-\text{H}\cdots\text{H}-\text{B}$ distances (2.11 Å in **1** vs 2.43 Å in **2**) and crystal packing motifs in these two systems attests to their widespread role in stabilizing the solid-state structures of hydrogen-rich materials. However, the geometrical properties of these novel interactions remain underexplored; whereas we have observed a spectrum of $\text{H}\cdots\text{H}$ distances associated with such behavior,⁵ nothing is known about the directionality that characterizes $\text{B}-\text{H}\cdots\text{H}-\text{B}$ bonding. Accordingly, we have conducted a statistical survey of the Cambridge Structural Database (CSD), which reveals a clear angular dependence for $\text{B}-\text{H}\cdots\text{H}-\text{B}$ interaction (Figure 3) that closely resembles the behavior of their more established $\text{N}-\text{H}\cdots\text{H}-\text{B}$ counterparts.^{2,13} The $\text{B}-\text{H}\cdots\text{H}$ angles from this survey cluster between 95 and 180 $^\circ$, indicating an ability to adopt either bent or linear geometries similar to proton-hydride interactions (ca. 65–180 $^\circ$). In contrast, traditional $\text{X}-\text{H}\cdots\text{Y}$ hydrogen bonds prefer a more linear mutual disposition of the donor and acceptor groups, placing $\text{B}-\text{H}\cdots\text{H}-\text{B}$ hydride-hydride bonding somewhere between these two extremes.¹ Moreover, the volume expansion experienced by a hydrogen atom attendant upon accumulation of negative charge indicates that 2.78 Å is a more plausible limit for the mutual overlap of the electron densities associated with the hydridic $\text{B}-\text{H}$ moieties in such hydride-hydride interactions.¹⁴ The expanded charge clouds of these hydridic species render neighboring $\text{B}-\text{H}$ bonds both *polarizable* and *polarizing* with respect to each other. Hence, while a first-order electrostatic interaction between two vicinal hydridic moieties is repulsive, second-order mutual polarization resulting from their distended charge clouds can plausibly account for the existence and surprising strength of these $\text{H}\cdots\text{H}$ interactions.

Analysis of the electron distribution in the vicinity of the shortest $\text{B}-\text{H}\cdots\text{H}-\text{B}$ contact in **2** clearly reveals a significant accumulation of electron density, $\rho(\mathbf{r})$, between the two hydrogen nuclei (Figure 4), showing that this homopolar dihydrogen bond is independent of the stronger $\text{Li}\cdots\text{H}-\text{B}$ interactions, in which the hydride moieties are polarized toward the Li^+ ions. Such a conclusion is also supported by the presence of a bond path (BP) and bond critical point (BCP) between the two $\text{B}-\text{H}$ moieties. The density observed at the BCP, $\rho_b(\mathbf{r})$ value, for this $\text{H}\cdots\text{H}$ interaction ($0.06 \text{ e}\text{\AA}^{-3}$) is approximately half that of its stronger $\text{Li}\cdots\text{H}-\text{B}$ counterparts ($0.10 \text{ e}\text{\AA}^{-3}$), confirming the secondary role of these hydride-hydride interactions in stabilizing the polymeric arrays in **2**. In contrast, the analogous hydride-hydride bonding in **1** was found to be similar in magnitude to its $\text{Li}\cdots\text{H}-\text{B}$ counterparts, emphasizing its more dominant role in the structure of this unsubstituted derivative.⁵ In spite of its secondary role in **2**, the

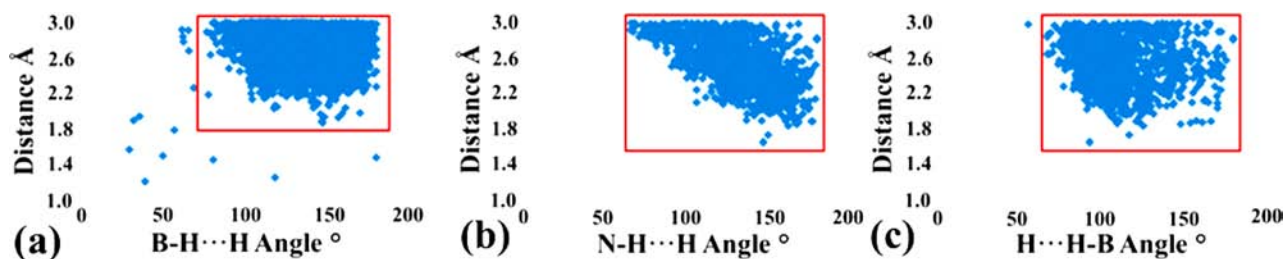


Figure 3. Statistical plots of the angle dependence for: (a) $\text{B}-\text{H}\cdots\text{H}-\text{B}$ contacts (7441 hits); and (b) and (c) $\text{N}-\text{H}\cdots\text{H}-\text{B}$ contacts (1135 hits), obtained from a survey of the CSD.

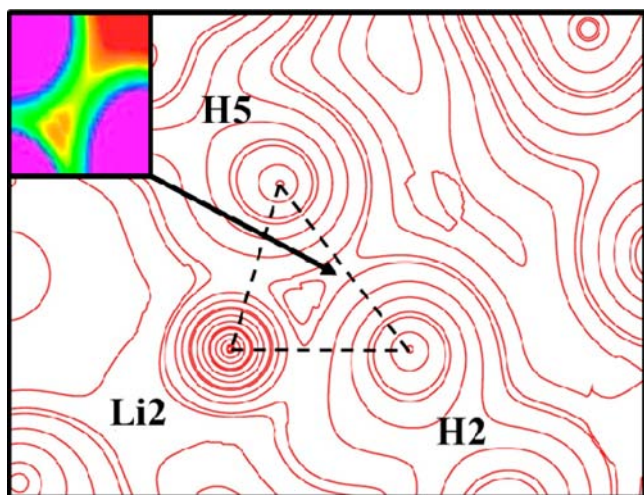


Figure 4. Calculated plot of the total electron density of $\text{LiNMe}_2\text{BH}_3$ (**2**) within the H2-Li2-H5 plane, highlighting the $\text{B1-H2}\cdots\text{H5}^\dagger-\text{B2}^\dagger$ contact and neighboring $\text{Li2}\cdots\text{H2-B1/Li2}\cdots\text{H5}^\dagger-\text{B2}^\dagger$ interactions. The contour levels increase in increments of 6.75×10^n , $1.35 \times 10^{n+1}$, $2.70 \times 10^{n+1}$, and $5.40 \times 10^{n+1} \text{ e}\text{\AA}^{-3}$ ($n = -3, -2, -1, 0, \text{ and } 1$) starting from the outermost contour inward. The valence electron density is shown in the upper left corner with yellow-to-green contours corresponding to densities of 0.05 and $0.07 \text{ e}\text{\AA}^{-3}$, respectively. \dagger denotes the crystallographic symmetry for the B2-H5 moiety as $x, 3/2 - y, 1/2 + z$.

$\rho_b(\mathbf{r})$ value for the hydride-hydride bonds still falls within the range of other weak intermolecular interactions commonly exploited in the engineering of molecular organic crystals.¹⁵

The polymeric chains in **2** are connected to each other along the a -axis through a multitude of weak homopolar $\text{C-H}\cdots\text{H-C}$ contacts, while the final dimension of the solid (b -axis) is stabilized through similar $\text{C-H}\cdots\text{H-B}$ interactions. It is notable that these $\text{H}\cdots\text{H}$ contacts exceed the sum of the VdW radii for two neutral hydrogen atoms (2.4 \AA ; q.v.).¹⁶ The weak nature of these interactions is also reflected in their electron distribution, as illustrated in the valence electron density plot projected along the a -axis of **2** (see Supporting Information), which shows no appreciable accumulation of electron density ($\leq 0.03 \text{ e}\text{\AA}^{-3}$) between the geminal N -methyl groups. Indeed, the $\rho_b(\mathbf{r})$ values for these heteropolar and homopolar dihydrogen interactions are considerably smaller than the strongest $\text{B-H}\cdots\text{H-B}$ bond in **2**, confirming that the polymeric units in this low-dimensional material are only weakly bound to one another through dispersion forces. Hence, the crystal structure of **2** is appropriately described as a supramolecular assembly with 1D directionality.

KNMe_2BH_3 (**3**) crystallizes in the same space group ($P2_1/c$; #14) as its lithium counterpart **2**. However, the greater size of K^+ results in significant changes to the primary and secondary interactions that stabilize its crystalline architecture. The cations in **3** adopt a pseudo-tetrahedral conformation with four coordinating $[\text{NMe}_2\text{BH}_3]^-$ anions. This gives rise to $\text{K}\cdots\text{H-B}$ and $\text{K}\cdots\text{N}$ interactions that form 2D polymeric layers (Figure 5), rather than the 1D chains observed in **2**. The greater size of K^+ also results in weaker inter-ion bonding, which in turn has a pronounced impact on the strength of the secondary interactions present in the structure. The $\text{B-H}\cdots\text{H-B}$ contacts (2.99 \AA) are again oriented in a zig-zag pattern, although the longer $\text{H}\cdots\text{H}$ separations preclude any stabilizing contribution to the polymeric layers. The lack of a stronger homopolar $\text{B-H}\cdots\text{H-B}$

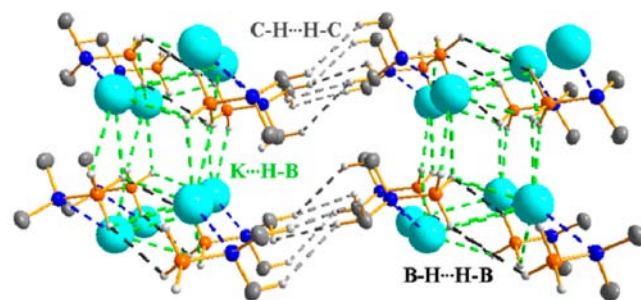


Figure 5. Extended structure of KNMe_2BH_3 (**3**), viewed in the ac plane of the crystal. Salient bond lengths (\AA) and angles ($^\circ$) are as follows: $\text{K}\cdots\text{N} = 2.81$; $\text{K}\cdots\text{H} = 2.74\text{--}2.91$; $\text{K}\cdots\text{H-B} = 84\text{--}108$; $(\text{B})\text{H}\cdots\text{H}(\text{B}) = 2.99$; $\text{B-H}\cdots\text{H} = 126\text{--}143$; $(\text{C})\text{H}\cdots\text{H}(\text{C}) = 2.40\text{--}2.76$; $\text{C-H}\cdots\text{H} = 113\text{--}169$.

$\text{H}\cdots\text{H-B}$ interaction in **3** does not reflect an inability of the B-H moieties to form hydride-hydride interactions; rather does the diffuse nature of the $\text{K}\cdots\text{H-B}$ and $\text{K}\cdots\text{N}$ bonding limit the extent of mutual polarization of these B-H groups.

The 2D polymeric layers in the ac plane of **3** engage all the B-H moieties of the $[\text{NMe}_2\text{BH}_3]^-$ anions, precluding the formation of additional stabilizing $\text{C-H}\cdots\text{H-B}$ interactions. In their absence, it falls upon weak $\text{C-H}\cdots\text{H-C}$ dispersion forces to hold together the sequential layers of this structure. The presence of weak homopolar dihydrogen bonding connecting the electrostatically bound ac layers of **3** leads us to characterize this system as a material with laminar, or 2D, directionality. This contrast with the linear 1D nature of **2**, and highlights how subtle changes in the chemical composition of a material can have a profound effect on the structure adopted in the solid state, where a multitude of weak interactions compete to determine the most favorable extended configuration. Having deliberately prevented the formation of conventional $\text{N-H}\cdots\text{H-B}$ proton-hydride interactions through N -methylation of the anions in **2** and **3**, their homopolar $\text{C-H}\cdots\text{H-C}$ counterparts step into the void and provide a surprising degree of supramolecular stability to these low-dimensional materials.

In summary, the stability of low-dimensional materials often relies on the presence of nonpolar layers or hydrophobic regions to direct the orientation of the molecules and/or ions within the framework of these soft crystals. This is exemplified in the solid-state structures of **2** and **3**, where inter-ion $\text{M}\cdots\text{N}$ and $\text{M}\cdots\text{H-B}$ interactions construct elaborate extended arrays that comprise the backbone of these structures. This generates the 1D and 2D directionality that defines these systems, and is reminiscent of the hydrogen bonding networks reported for liquid crystals and hybrid inorganic-organic polymers.^{17,18} These structural motifs are then supported by constrained $\text{B-H}\cdots\text{H-B}$ hydride-hydride contacts that result from the mutual polarization of the B-H moieties. These homopolar $\text{H}\cdots\text{H}$ interactions play a secondary role in stabilizing the polymeric units in **2**, as reflected by their moderate accumulation of electron density. In contrast, the weaker nature of the primary ionic bonding in **3** limits the mutual polarization of the B-H moieties, effectively preventing any significant $\text{B-H}\cdots\text{H-B}$ bonds from being formed. Finally, the geminal N -methyl groups (i.e., nonpolar layers) that form a sheath around the polymeric arrays in **2** and **3** ensure that only weak secondary $\text{H}\cdots\text{H}$ interactions can determine the most favorable extended structures for these systems. We anticipate that other molecular hydrides in which proton-hydride bonding is frustrated

through the deliberate alkylation of N–H (or O–H) moieties will show a similar proclivity to resort to homopolar dihydrogen interactions as a replacement. Such a strategy also offers an attractive novel approach for deliberately constructing and stabilizing low-dimensional crystal architectures.

■ ASSOCIATED CONTENT

● Supporting Information

Complete details of the synthesis and characterization of $\text{LiNMe}_2\text{BH}_3$ (2) and KNMe_2BH_3 (3), along with the geometrical and topological parameters for the individual interactions in these systems. This material is available free of charge via the Internet at <http://pubs.acs.org>.

■ AUTHOR INFORMATION

Corresponding Author

dwolsten@unb.ca; smcgrady@unb.ca

Notes

The authors declare no competing financial interest.

■ ACKNOWLEDGMENTS

We are grateful to the Natural Sciences and Engineering Research Council of Canada (NSERC) and the New Brunswick Innovation Foundation (NBIF) for financial support of this research.

■ REFERENCES

- (1) Steed, J. W. *Supramolecular Chemistry*; John Wiley & Sons, Ltd.: West Sussex, U.K., 2000.
- (2) (a) Brown, M. P.; Heseltine, R. W. *Chem. Commun.* **1968**, 1551–1552. (b) Lee, J. C.; Rheingold, A. L.; Muller, B.; Pregosin, P. S.; Crabtree, R. H. *J. Chem. Soc., Chem. Commun.* **1994**, 1021–1022. (c) Lough, A. J.; Park, S.; Ramachandran, R.; Morris, R. H. *J. Am. Chem. Soc.* **1994**, *116*, 8356–8357. (d) Richardson, T. B.; de Gala, S.; Crabtree, R. H.; Seighan, P. E. M. *J. Am. Chem. Soc.* **1995**, *117*, 12875–12876. (e) Custelcean, R.; Jackson, J. E. *Chem. Rev.* **2001**, *101*, 1963–1980.
- (3) (a) Matta, C. F.; Hernández-Trujillo, J.; Tang, T.-H.; Bader, R. F. W. *Chem.—Eur. J.* **2003**, *9*, 1940–1951. (b) Wolstenholme, D. J.; Cameron, T. S. *J. Phys. Chem. A* **2006**, *110*, 8970–8978. (c) Wolstenholme, D. J.; Matta, C. F.; Cameron, T. S. *J. Phys. Chem. A* **2007**, *111*, 8803–8813. (d) Echeverría, J.; Aullón, G.; Danovich, D.; Shaik, S.; Alvarez, S. *Nat. Chem.* **2011**, *3*, 323–330.
- (4) Eisenschitz, R.; London, F. Z. *Phys.* **1930**, *60*, 491–527.
- (5) Wolstenholme, D. J.; Titah, J. T.; Che, F. N.; Traboulsee, K. T.; Flogeras, J.; McGrady, G. S. *J. Am. Chem. Soc.* **2011**, *133*, 16598–16604.
- (6) Wolstenholme, D. J.; Traboulsee, K. T.; Hua, Y.; Calhoun, L. A.; McGrady, G. S. *Chem. Commun.* **2012**, *48*, 2597–2599.
- (7) Sirsch, P.; Che, F. N.; Titah, J. T.; McGrady, G. S. *Chem.—Eur. J.* **2012**, *18*, 9476–9480.
- (8) Guerra, D.; David, J.; Restrepo, A. *Phys. Chem. Chem. Phys.* **2012**, *14*, 14892–14897.
- (9) Chen, X.; Yuan, F.; Tan, Y.; Tang, Z.; Yu, X. *J. Phys. Chem. C* **2012**, *116*, 21162–21168.
- (10) Bader, R. F. W. *Atoms in Molecules: A Quantum Theory*; Oxford University Press: Oxford, U.K., 1990.
- (11) Aldridge, S.; Downs, A. J.; Tang, C. Y.; Parsons, S.; Clarke, M. C.; Johnstone, R. D. L.; Robertson, H. E.; Rankin, D. W. H.; Wann, D. A. *J. Am. Chem. Soc.* **2009**, *131*, 2231–2243.
- (12) (a) Xiong, Z.; Yong, C. K.; Wu, G.; Chen, P.; Shaw, W.; Karkamkar, A.; Autrey, T.; Jones, M. O.; Johnson, S. R.; Edwards, P. P.; David, W. I. F. *Nat. Mater.* **2008**, *7*, 138–141. (b) Wu, H.; Zhou, W.; Yildirim, T. *J. Am. Chem. Soc.* **2008**, *130*, 14834–14839.

(13) Bruno, I. J.; Cole, J. C.; Edgington, P. R.; Kessler, M.; Macrae, C. F.; McCabe, P.; Pearson, J.; Taylor, R. *Acta Crystallogr.* **2002**, *B58*, 389–397.

(14) Lang, P. F.; Smith, B. C. *Dalton Trans.* **2010**, *39*, 7786–7791.

(15) (a) Koch, U.; Popelier, P. L. A. *J. Phys. Chem.* **1995**, *99*, 9747–9754. (b) Popelier, P. L. A. *J. Phys. Chem. A* **1998**, *102*, 1873–1878. (c) Mallinson, P. R.; Smith, G. T.; Wilson, C. C.; Grech, E.; Wozniak, K. *J. Am. Chem. Soc.* **2003**, *125*, 4259–4270. (d) Zhurova, E. A.; Stash, A. I.; Tsirelson, V. G.; Zhurov, V. V.; Bartashevich, E. V.; Potemkin, V. A.; Pinkerton, A. A. *J. Am. Chem. Soc.* **2006**, *128*, 14734–14734. (e) Munshi, P.; Cameron, E.; Row, T. N. G.; Ferrara, J. D.; Cameron, T. S. *J. Phys. Chem. A* **2007**, *111*, 7888–7897.

(16) (a) Bondi, A. *J. Phys. Chem.* **1964**, *68*, 441. (b) Nyburg, S. C.; Faerman, C. H. *Acta Crystallogr., Sect. B* **1985**, *41*, 274–279.

(17) Lagerwall, J. P. F.; Scalia, G. *Curr. Appl. Phys.* **2012**, *12*, 1387–1412.

(18) Kawakami, Y.; Li, Y.; Liu, Y.; Seino, M.; Pakjamsai, C.; Oishi, M.; Hee, Y.; Imae, I. *Macromol. Res.* **2004**, *12*, 156–171.